Development of Bainitic Steels for Engineering Applications

V. C. Igwemezie, P. C. Agu
Department of Materials & Metallurgical Engineering
Federal University of Technology, Owerri

***Abstract*— Enormous efforts have been put in in an attempt to design steel with microstructure in the Nano range. Phase transformation theory has contributed to the successful design of these steels. This paper presents some of these developments, the physical metallurgy theory involved and areas where these materials have been destined.**

Keywords*— phase transformations, bainitic steel, engineering application*

I. INTRODUCTION

The development of bainitic steel was based on making small grain size steel smaller in the hope of finding novel high strength and tough steel for advancement of technology. The increasing need for these materials has led to development of theories, models, software, and practices which are now of immense value in the design of steel. Novel iron alloys are being conceived, manufactured, and marketed with a regularity which has confounded many prophecies [1].

The world stood still recently as the first bulk nanostructured metal was produced by Tata Steel and Rolls Royce Plc [2]. This underscores the strategic position of steel in propelling technology. Iron gives diverse range of properties and phenomena when a small amount of alloying element is added. An addition of just carbon to iron leads to formation of microstructures with varied properties. These properties are not invariant to changes in dimensions, which broadens the manoeuvrability of the material.

When steel is heated above, say 910 $^{\circ}C$, it develops the face-centred cubic crystal structure which is more commonly known as austenite (γ) (Figure 1.1(a)). The austenite on cooling undergoes a solid-state transformation into the body-centred cubic crystal structure known as ferrite (Figure 1(b).

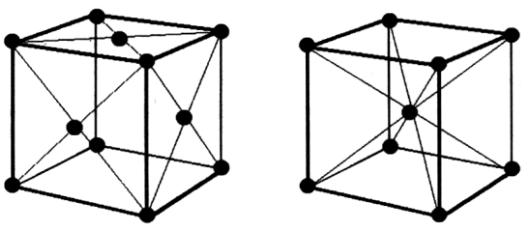

(a) (b)

Figure 1.1: The two common crystal structures of iron; (a) *fcc austenite* (b*) bcc ferrite*. (For clarity, only three of the six face-centring atoms of austenite are shown)

The transformation from austenite to ferrite can occur by a variety of atomic mechanisms [3]. The pattern in which the atoms are arranged can be altered either by breaking all the bonds and rearranging the atoms into an alternative pattern termed reconstructive transformation or by homogeneously deforming the original pattern into a new crystal structure termed displacive transformation [3]. Figure 1.2 shows how these two mechanisms can take place.

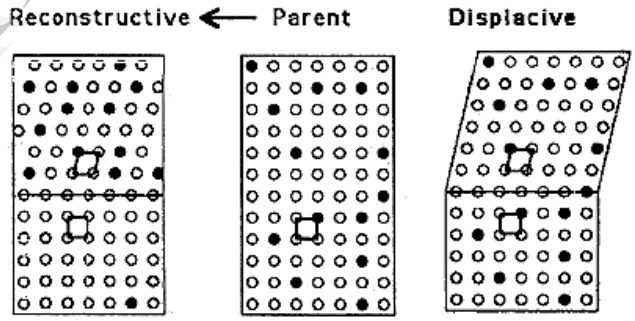

Figure 1.2: The reconstructive and displacive atomic mechanisms of transformation [4].

The development of bainitic steel has been centred on bainite microstructure which undergoes displacive transformation.

.

II. DISPLACIVE TRANSFORMATION

Displacive transformation is characterised by a well-coordinated movement of atoms in which the atomic correspondence between the parent and product phases is preserved (Figure 1.2) [4]. In other words, the deformation carries the parent into the product phase. This occurrence, changes the overall shape of the sample. That is it leads to a macroscopic change in shape of the sample when the product phase is not constrained. In a polycrystalline material involving several grains adjacent to each other this product phase grows in the form of thin plates which is a morphology which reduces the strain energy associated with this transformation mechanism [5]. Displaci.ve transformations can occur at temperatures where diffusion becomes impossible over the

time scale of the experiment. Some solutes may be forced into the product phase, a phenomenon known as solute trapping. Both the trapping of atoms and the strains make displacive transformations less favourable from a thermodynamic point of view [6]. The shapes adopted by the crystals due to this displacive transformation are classed as Widmanstätten ferrite, Bainite and Martensite. This paper focuses on the exploitation of Bainite transformation mechanism in the development and commercialisation of strong bainitic steel.

III. THE BAINITE TRANSFORMATION

Bainite (α_b) is found to consist of a non-lamellar aggregate of carbides and plate-shaped ferrite [5, 7]. The highest temperature at which bainite can form in a steel of fixed composition is referred to as the bainite start temperature, B_S and that of martensite-start temperature as M_S [2].The determination of these start temperatures can be found in [8, 9].

When an austenite is cooled below B_S, bainite is nucleated and grows in form of a thin plate. The plate results in order to minimize strain energy. The excess carbon in the newly formed bainitic ferrite is subsequently partitioned into the remaining austenite enriching it. Given time, this carbon-enriched austenite decomposes into a mixture of cementite and ferrite as shown in Figure 3.1 [10, 11]. Substitutional solutes do not partition during any stage in the formation of bainite [14]

Why the partitioning of excess carbon? The maximum solubility of carbon in ferrite that is in equilibrium with austenite is about little above $0.02\ wt\%$ at a temperature of about $600°C$ due to the retrograde shape of the $\alpha/\alpha + \gamma$ phase boundary [2]. Despite the partitioning of carbon, more carbon against the equilibrium amount for ferrite is retained by the bainitic ferrite. This carbon fails or is reluctant to partition into the residual austenite in spite of the fact that the process is not limited by atomic mobility, even under prolonged heat treatment [2].

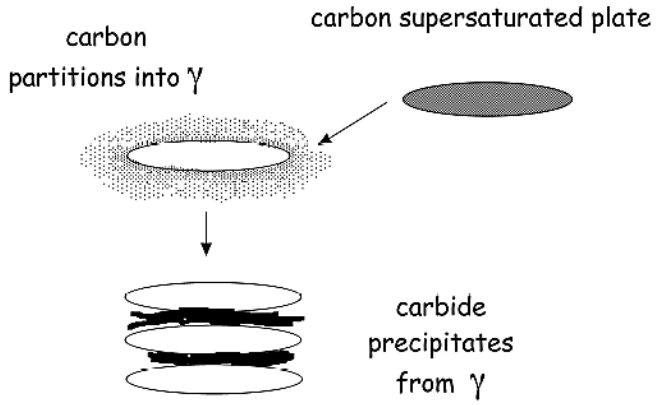

Figure 3.1: Stages in the formation of upper bainite [11].

Studies have shown that the excess carbon in the bainitic ferrite can be found at dislocations and grain boundaries where they are trapped and at defect-free solid solution. The latter position rules out solute trapping by defects as the sole culprit for the retention of the extra carbon. The explanation given [2] is that the presence of carbon in the bainitic ferrite changes ferrite crystal structure from normal body-centred cubic, bcc to body-centred tetragonal ferrite, bct. The bct structure changes the symmetry of the ferrite thereby altering the thermodynamic equilibrium. The amount of carbon, trapped can be up to 0.30 wt.%.This phenomenon adds to the strengthening of the steel [36].

Thermodynamic data were calculated using *ab initio* methods, and subsequently incorporated into phase diagram calculations [2]. Figure 3.2 shows the result of that exercise. The graph indicates that the solubility of carbon in tetragonal ferrite in equilibrium with austenite is much larger than that for cubic ferrite.

Bainite grows at temperatures where the austenite is mechanically weak and unable to elastically accommodate the shape deformation accompanying transformation. The shape deformation is accommodated by plastic relaxation of the surrounding austenite. Consequently, dislocations are generated during the plastic deformation at the adjacent austenite causing a loss of coherency at the α_b/γ interface [12]. This loss of coherency halts the growth of the bainite platelets before it encounters any hard obstacle such as austenite grain boundary. This is illustrated by the sub–unit mechanism of bainite (Figure 3.3). For the transformation to continue, new platelets nucleate and grow giving rise to clusters of parallel sub-units with identical crystallographic orientation, habit plane and size as shown in Figure 3.3 [3]. Not only does this mechanism lead to solute trapping but also a huge strain energy term, both of which reduce the heat of transformation [14]. The growth of individual plates is fast and the rate of transformation of bainite is controlled by nucleation rather than growth

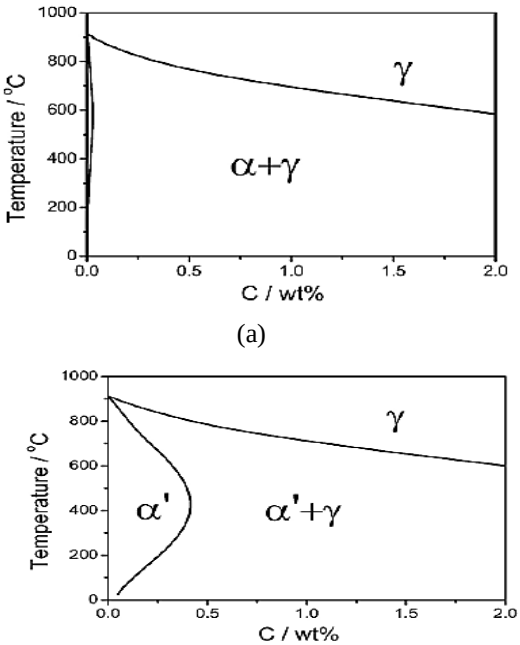

Figure 3.2: Binary phase diagram of the Fe–C system allowing (a) equilibrium between bcc ferrite and austenite, (b) between bct ferrite and austenite [2].

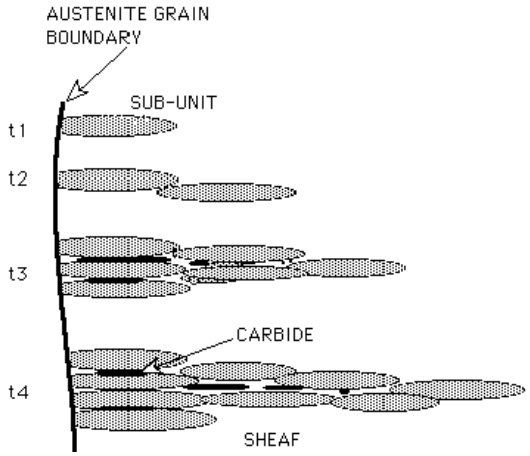

Figure 3.3: Evolution of a bainite sheaf as a function of time.

Bainite is generally classified into two forms - the upper bainite and lower bainite. In the upper case, a plate of bainite forms without diffusion, but any trapped or excess carbon then partitions into the residual austenite where it eventually precipitates as cementite. Conventional upper bainite consists of a non-lamellar mixture of bainitic ferrite plates with intervening particles of cementite [10].

The upper bainite appears as clusters of platelets of ferrite in identical crystallographic orientation and intimately connected to the austenite in which they grow. As already mentioned above, elongated cementite particles decorate the boundaries of these platelets, the amount and continuity of the cementite layers depending on the carbon concentration of the steel.

As the transformation temperature is reduced, some of the carbon is encouraged to precipitate inside the supersaturated bainitic ferrite, giving rise to the lower bainitic microstructure [7]. Figure 3.4 shows the summary of the mechanism of bainite transformation.

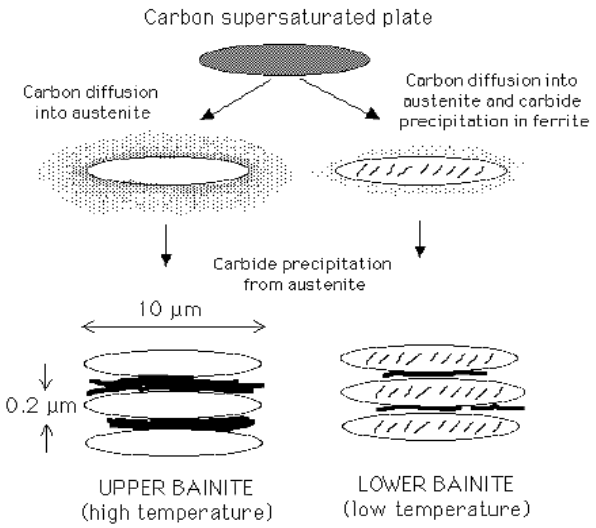

Figure 3.4: Summary of the mechanism and microstructure of bainite in steels [7, 10, 13].

The bainitic ferrite clusters are known as sheaves. Each ferrite plate is about $10\mu m$ long and about $0.2 \times 10^{-6}\ m$ thick (Figure 3.4), making an individual plate invisible in the optical microscope. The fine scale of the microstructure is beneficial to both the strength and toughness [7].

As already mentioned above, the transformation of austenite into bainite leads to a shape deformation which is found to be macroscopically an invariant plane strain (IPS) with a large shear component, as illustrated in Figure 3.5.

What is IPS? When bainite forms, there is conservative glide of a dislocation on a slip plane which causes shear in a direction which lies in that plane. The material in the slip plane remains crystalline during the deformation, with no change in the relative positions of atoms on that plane, which is said to be invariant to the strain. This phenomenon is usually referred to as IPS. Figure 3.5 (a)1 illustrates an invariant–plane strain (IPS) which is dilatational, and is of the type to be expected when a plate–shaped precipitate grows diffusionally. The change of shape is due to the volume change accompanying transformation. In Figure 3.5 (a) 2, the IPS corresponds to a simple shear at constant volume, as in slip or mechanical twinning.

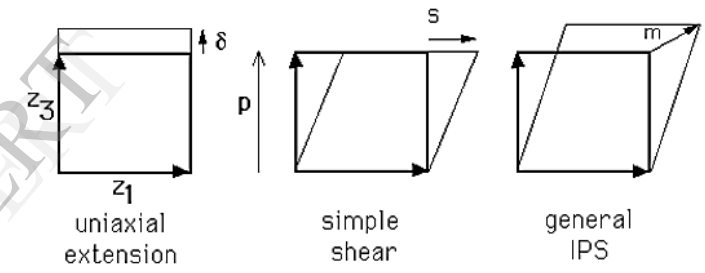

(a)

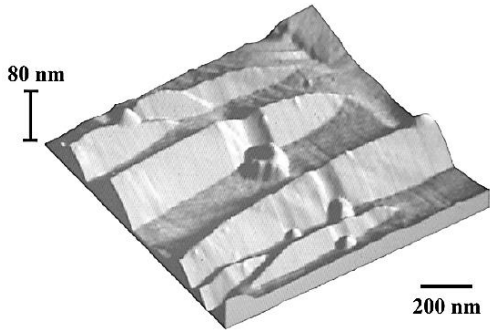

1 **2** **3**

(b)

Figure 3.5: (a) Three kinds of invariant–plane strains. The squares indicate the shape before deformation. δ, s and m represent the magnitudes of the dilatational strain, shear strain and general displacement respectively. p is a unit vector, the shear strain s is parallel to $z1$, whereas δ is parallel to $z3$. (b) A sample of steel polished flat, austenitized and then transformed into bainitic ferrite, resulting in large disturbances of the surface, representing a shear

strain of ≈0.46 and a dilatational strain normal to the habit plane of 0.03 [2].

In general, IPS is a combination of dilatation and shear. Figure 3.5 (a) 3 illustrates the shape deformation accompanying the formation of bainite or martensite, with $s \cong 0.22-0.26$ and $\delta \cong 0.02-0.03$. These deformations are found to be much larger than elastic strains in a tensile test, which are of the order of 0.001. Hence, s and δ have profound effects on the properties of bainitic steel.

It is found that the crystallography of the low-temperature bainite platelets is such that there is an exceptionally large shear strain of ≈ 0.46 accompanying transformation, which compares with bainite formed at elevated temperatures where the strain is ≈ 0.26 [2]. The larger the shear strains the thinner or finer the bainitic plates. In other words, the lower the transformation temperature the thinner the bainitic plates.

IV. CARBIDE–FREE BAINITE

The early problem of this bainitic microstructure is that it has brittle cementite. The cementite is detrimental to engineering properties. It makes the steel prone to cleavage fracture and void formation. It is found that by increasing the amount of silicon, Si in the steel, a bainite microstructure free of carbide can be obtained [11]. During transformation the carbon that is rejected into the residual austenite instead of precipitating as cementite, remains in the austenite and stabilises it down to ambient temperature. The resulting microstructure consists of fine plates of bainitic ferrite separated by carbon–enriched regions of austenite. Figure 4.1 shows the much celebrated carbide free bainitic microstructure.

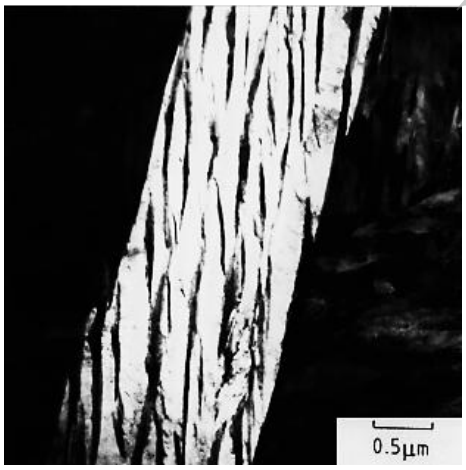

Figure 4.1: Transmission electron micrograph of a sheaf of Carbide-free upper bainite, consisting of fine ferrite platelets separated by films of carbon–enriched retained austenite [7, 11, 15].

The advantages of this carbide free, mixed microstructure of bainitic ferrite and austenite are [7, 11]:

- Elimination of Brittle cementite which makes the steel more resistant to cleavage fracture and void nucleation,
- Resistant to tempering as its strength is not derived from dissolved carbon. Dissolved carbon embrittles the ferrite The bainitic ferrite is depleted in carbon which toughens the steel.
- The presence of the fine plates of ferrite confers strength and refinement is the only mechanism for simultaneously improving the strength and toughness of steels.
- The austenite films which are intimately dispersed between the plates of ferrite are ductile and so stand as barriers to the propagation of cracks. That is they have a crack blunting effect. Austenite also is a barrier to the diffusion of hydrogen.
- The diffusion of hydrogen in austenite is slower than in ferrite. Austenite can therefore lead to an improved stress–corrosion resistance.
- Steels with this microstructure are cheap. All that is required is that the silicon concentration should be large enough to suppress cementite. The simple heat treatment needed to generate the microstructure gives a fine structure which will require complex processing to achieve with other methods.

An important feature of bainite formation is that at the low temperature, diffusion distance of an iron atom is an inconceivable 10^{-17} over the time scale of the experiment and there is no redistribution of substitutional atoms on the finest conceivable scale [14]. The retained austenite after transformation is in two forms, the desirable films between the fine plates of ferrite Figure 4.1 and blocks between different crystallographic variants of bainite, Figure 4.2. As a result, two distinct peaks are usually seen with each austenite reflection in synchrotron X-ray diffraction experiments as transformation evolves [14].

The initial pitfall of this carbide-free bainitic ferrite/austenite is that it lacked good combination of strength and toughness due to retention of large "blocky" regions of austenite between the sheaves of bainite (Figure 4.2). The blocks of austenite are the consequence of suppression of formation of the brittle cementite and are unstable.

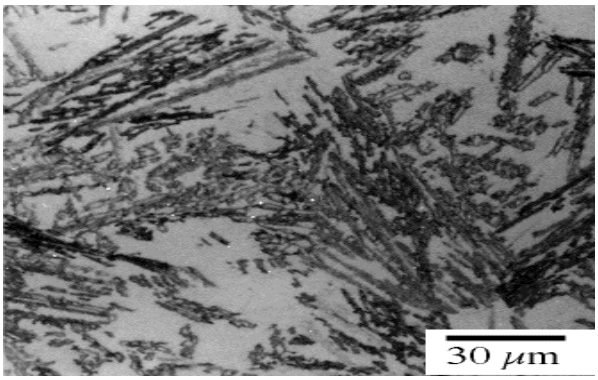

Figure 4.2: Optical micrograph of upper bainite in an $Fe-0.43C-3Mn-2.02Si\ wt.\%$ showing the blocks of retained austenite between sheaves of bainite. [7, 15]

The problem is that the size of the Blocks of retained austenite is coarser than desired. The blocky regions are less stable and transform into high–carbon martensite under the influence of a small applied stress. This untempered, hard martensite embrittles the steel compromising its mechanical properties. To solve this problem, it was proposed that anything that can be done to reduce the blocky austenite size, or to increase their stability to avoid martensitic transformation, is expected to be beneficial.

As discussed above, bainite grows without diffusion, but that the excess carbon is soon afterwards partitioned into the residual austenite. It is found that diffiusionless growth cannot be sustained once the carbon concentration of the austenite reaches the T_o $curve$ of the phase diagram, i.e., x_{T_o} as shown in Figure 4.3. In other words Diffusionless transformation is thermodynamically impossible if the carbon concentration of the austenite exceeds the T_o curve. T_o $curve$ is the locus of points where austenite and ferrite of the same composition have identical free energies

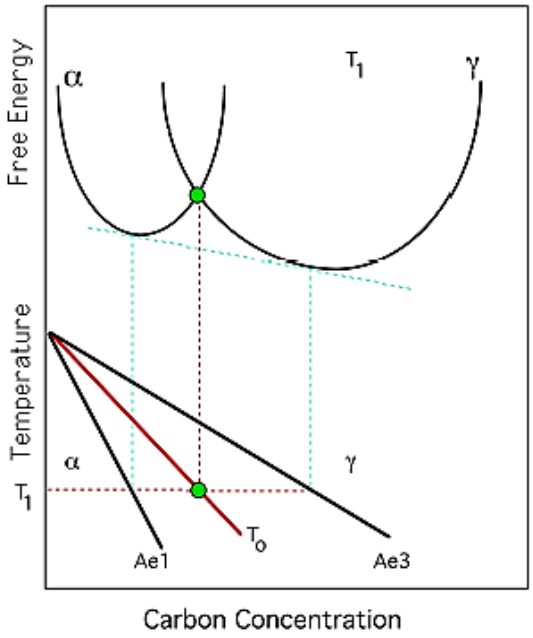

Figure 4.3: Illustration of the origin of the T_o construction on the Fe–C phase diagram. Diffusionless transformation is thermodynamically impossible if the carbon concentration of the austenite exceeds the T_o curve [7, 11].

Diffusionless growth requires that transformation occurs at a temperature below a temperature T_o, when the free energy of bainite becomes less than that of austenite of the same composition as shown in Figure 4.3 [11, 13]. In other words growth without a composition change can only occur if the carbon concentration of the austenite lies to the left of the T_o curve.

Bainitic ferrite formation is accompanied by strain energy. This strain energy is usually accounted for by raising the free energy curve of the ferrite by a quantity equal to the strain energy, thus defining the T_o' curve which occurs at slightly lower carbon concentrations with $T_o' < T_o$. In bainitic transformation it is estimated to be $G_{SB} \cong 400\, J\, mol^{-1}$. Figure 4.4 is a typical treatment of bainitic transformation mechanism.

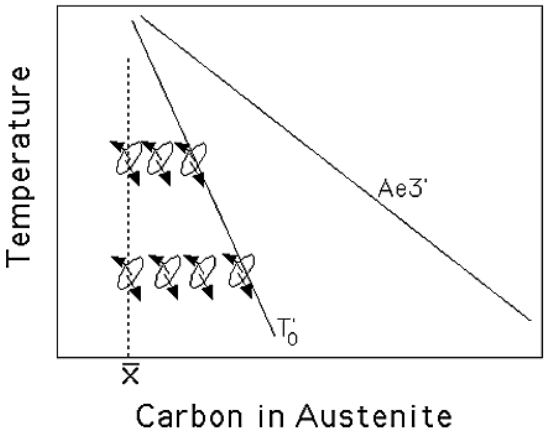

Figure 4.4: The incomplete reaction phenomenon of bainite formation [10].

The maximum fraction of bainite that can form in the silicon–rich steel is given by the application of the lever rule to the T_o' curve thus (Figure 4.5) [7];

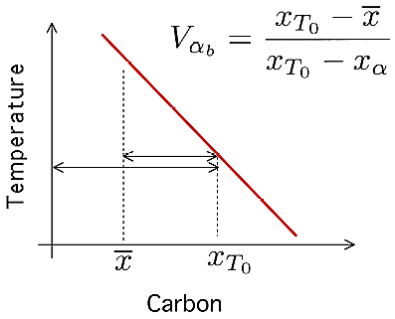

Figure 4.5: Lever rule applied to the T_o curve to determine the permitted fraction of bainite [11].

$$V_{\alpha_b}^{max} = \frac{x_{T_o'} - \bar{x}}{x_{T_o'} - x_\alpha}$$

where $x_{T_o'}$ is the carbon concentration given by the T_o' boundary, $\bar{x}$ is the mean carbon concentration of the alloy, and $x_\alpha \cong 0$ is the carbon concentration left in the ferrite. Increase in $V_{\alpha_b}^{max}$ leads to a reduction in blocky austenite and an increase in the stability of the remaining austenite. Modifying the alloy system with substitutional solute to shift T_o' curve to higher carbon concentrations or increase in x_{T_o} led to reduction of the troublesome blocks of retained austenite. In other words addition of a substitutional element causes reduction ΔT_o in the T_o temperature permitting more bainitic ferrite to form.

This alteration in composition which increases in the T_o' curve, leading to a decrease in the amount of blocky austenite causes a remarkable improvement in toughness without sacrificing strength [7, 15]. In this way combination of strength and toughness of $1600\, MPa$ and $130 MPam^{\frac{1}{2}}$ respectively

have been achieved [16, 17]. It is reported that these properties compare with those of the nickel and molybdenum-rich marageing steels at a cost some ninety times cheaper [11].

V. SOME DESIGN ISSUES

The nucleation stage of bainite involves the partitioning of carbon so the chemical free energy change (ΔG_m) for this stage is larger; the magnitude of this driving force must exceed a value prescribed by a function $|G_N|$ in order to obtain a detectable nucleation rate [19]. B_s is defined when both the nucleation and the growth conditions are satisfied simultaneously. That is

$$\underbrace{\Delta G_m < G_N}_{nucleation\ \ condition} \quad and \quad \underbrace{\Delta G^{\gamma\alpha} < -G_{SB}}_{growt\ h\ condition} \qquad (5.1)$$

Martensitic transformation occurs when $\Delta G^{\gamma\alpha}$ becomes less than a critical value $\Delta G^{\gamma\alpha}\{M_s\}$ given by the function $G_N^{\alpha'}$

$$\Delta G^{\gamma\alpha} < G_N^{\alpha'} \qquad (5.2)$$

$G_N^{\alpha'}$ is taken to be approximately constant value for low alloy steels while a function dependent on the strength of the austenite is used for steels containing large concentrations of solute.

Bainite structure can be refined by reducing the transformation temperature [2, 24-27, 33].The chemical free energy change accompanying the diffusionless growth of either bainite or martensite when neglecting all the stored energy terms is given as [19].

$$\Delta G^{\gamma\alpha} = G^{\alpha} - G^{\gamma} \qquad (5.3)$$

In other words the difference in the free energy between austenite and ferrite ($\Delta G^{\gamma\alpha} = G^{\alpha} - G^{\gamma}$) is the driving force for transformation. G is the Gibbs free energy, α and γ are the product and parent phases, respectively. The nucleation and growth rates of bainitic phase increase as a function of $|\Delta G^{\gamma\alpha}|$.

Since bainite and martensite are not equilibrium transformations, there is energy stored inside the steel, as a consequence of their transformation, in the form of elastic strains. This stored energy is usually accounted for in steel design. As already mentioned, in the case of bainite, this is given as $G_{SB} \cong 400\ J\ mol^{-1}$ [34].

This theory was used to estimate the lowest temperature at which bainite can form in $Fe-2Si-3Mn\ steel$. The result of the finding is shown in Figure 5.1. Figure 5.1(a), shows how the B_s and M_s temperatures vary as a function of the carbon concentration. It suggests that in principle no lower limit to the temperature at which bainite can be generated [14]. In other words, bainite can be formed at room temperature.

Figure 5.1(b) shows that the rate of bainite formation slows down dramatically as the transformation temperature is reduced. It implies that to generate bainite at room temperature, one has to wait for hundreds or thousands of years.

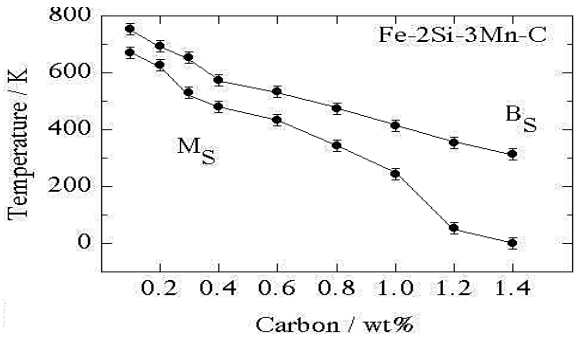

(a)

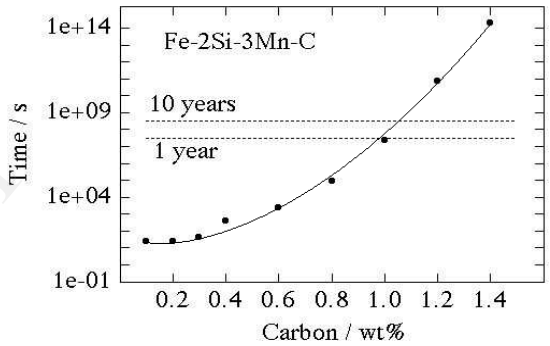

(b)

Figure 5.1: (*a*) Calculated bainite-start (B_s) and martensite-start (M_s) temperatures as a function of the carbon concentration in $Fe-2Si-3Mn\ steel$. (*b*) The calculated time required to initiate bainite at the B_s temperature as a function of the carbon concentration [8, 14, 19, 32].

Carbon are found to be much more effective in maintaining a difference between the B_s and M_s temperatures than are substitutional solutes which reduce $|\Delta G^{\gamma\alpha}|$ simultaneously for martensite and bainite. This calculated bainite and martensite-start temperatures is shown in Figure 5.2.

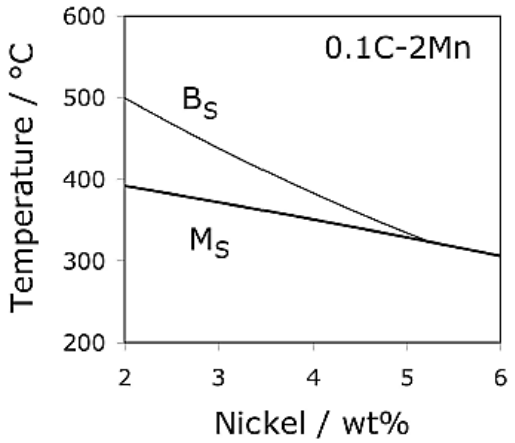

(a)

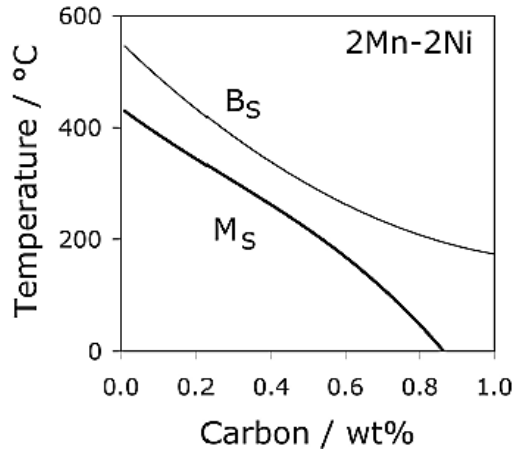

(b)

Figure 5.2: Calculated B_s and M_s temperatures: (a) $Fe-0.1C-2Mn\ wt\%$, with a variation in nickel concentration; (b) $Fe-2Ni-2Mn$ with a variation in the carbon concentration [14].

The carbon partitioning during transformation allows bainite to form at a higher temperature than martensite. This advantage is found to diminish as the overall carbon concentration is reduced, as illustrated in Figure 5.2 (b) [14].

Above theories and principles were integrated into a mechanism–based model, leading to the design of novel bainitic steels with a carbide–free bainitic microstructure as discussed below.

A typical system for this class of steels is given below and here referred to as **Alloy System 1**

$$Fe-0.98C-1.46Si-1.89Mn-0.26Mo-1.26Cr-0.09V\ wt\%$$

Manganese and chromium are added to increase hardenability, and silicon to prevent cementite precipitation. The molybdenum is added to prevent prior austenite grain boundary embrittlement (temper embrittlement) due to phosphorus [28, 29, 30]. The substitutional solutes also contribute to hardenability and determine the T_o curve which is vital in the design of carbide-free bainitic steels.

However, producing at this very slow rate, running into months cannot be exciting and has disadvantages in relation to economy of rapid production rate, hence the need to find a way to accelerate the transformation kinetics. The transformation is found to easily accelerate within hours, by adding solutes which decrease the stability of austenite [14]. Study shows that addition of cobalt and aluminium in concentrations less than 2 wt%, accelerate the transformation by boosting $|\Delta G^{\gamma\alpha}|$. The increase in the rate of transformation is shown in Figure 5.3. Both are said to be effective, either on their own or in combination [26].

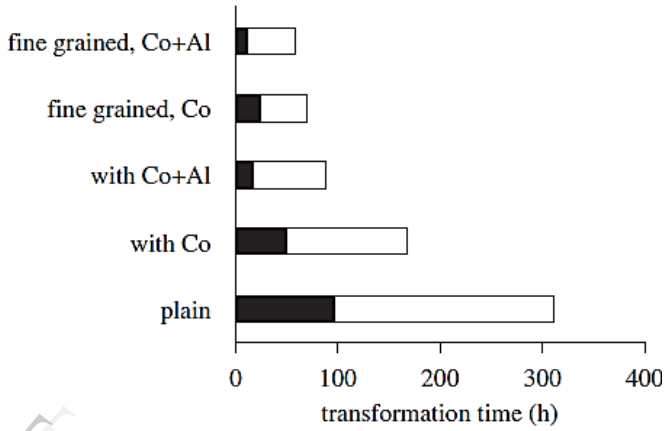

Figure 5.3: Time taken for carbide-free reaction to start and to terminate during isothermal heat treatment at $200°C$ of the **Alloy System 1** and others with $1.5\ wt\%\ Co$ or a combined addition of $1.5Co$ and $1Al\ wt\%$. Black bars, begin; white bars, end [19, 26].

Alloy System 1 was transformed at $200°C$ by isothermal transformation to obtain bainite while avoiding martensitic transformation. The result is an elegant, amazing and celebrated microstructure shown in Figure 5.4. The structure consists of slender plates of bainite dispersed in stable carbon-enriched austenite *(γ)* (retained austenite – the parent phase) only $200-400Å$ *(20–40 nm)* thick. The fcc lattice is found to mount formidable barrier to crack propagation [21, 14, 24, 25-26, 35].

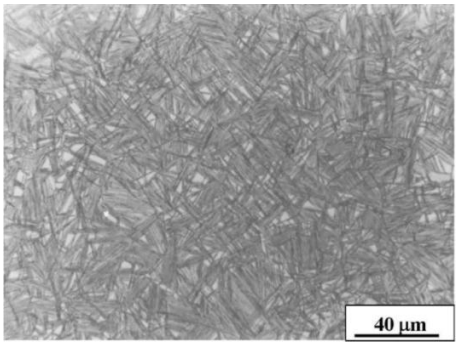

(a)

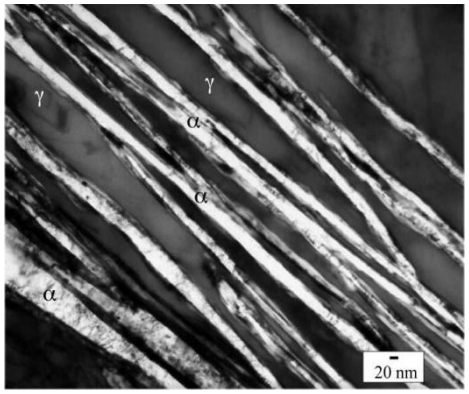

(b)

Figure 5.4:

$Fe - 0.98C - 1.46Si - 1.89Mn - 0.26Mo - 1.26Cr - 0.09V\ wt\%$, transformed at $200℃$ for 5 days. (a) Optical micrograph.

(b) Transmission electron micrograph. [2, 14, 18, 19, 21, 24, 25, 35].

The scale of the microstructure, i.e., the thickness of the bainite plates, decreases as the transformation temperature is reduced This is because the yield strength of the austenite becomes greater at lower temperatures, thereby affecting the plastic accommodation of the shape deformation accompanying bainite growth, and presumably because the nucleation rate can be greater at larger undercoolings [14].

As already mentioned, the increase in strength in microstructures generated at lower temperatures is attributed to the extremely thin platelets of bainitic ferrite (very small thickness of the bainite plates) generated at low temperature. In general, as the transformation temperature is reduced the strength of the austenite increases and the plates of bainite get finer [7, 37].

Theory indicates that the contribution to strength due to the size of the plates is given by [36]

$$\Delta\sigma \cong \mathbf{115}(\bar{L})^{-1}\ (MPa)$$

where $\bar{L} \cong 2t$.

$\bar{L}$ is the mean lineal intercept in micrometres and t the true thickness of the bainitic ferrite. And so, for plates thickness of 30 nm $\Delta\sigma \cong 1916\,MPa$, whereas $\Delta\sigma \cong 898\,MPa$ for a plate thickness of 64 nm at transformation temperature of $300℃$. This theory shows that strength of the microstructure scales with the inverse of the plate thickness. In other words, the strength varies linearly with the reciprocal of the ferrite plate thickness.

VI. Engineering Properties of Designed Bainitic Steels

In practice, the mean linear intercept $\bar{L}$ depends on the fraction of bainite V_b. If plates are assumed to be square then $(\bar{L})^{-1} \propto V_b/t$. The relationship of UTS, and YS to the ratio V_b/t, is shown in Figure 6.1 using The **Alloy System 1** transformed at $200℃$.

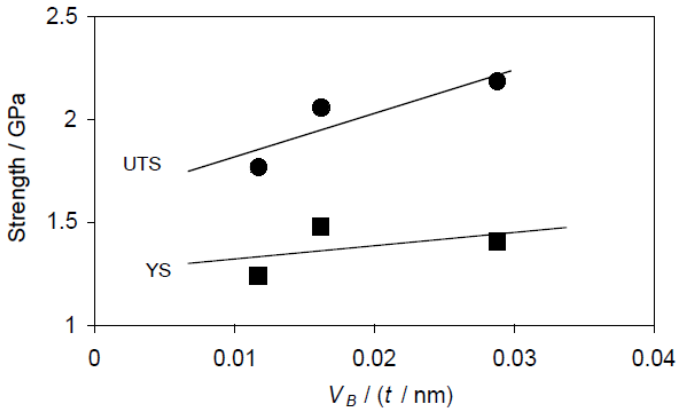

Figure 6.1: Strength versus V_b/t [36].

Figure 6.2: shows an inverse relationship of hardness on plate thickness of the bainitic alloy system (1) mentioned above. This implies that hardness increases as the bainitic plate thickness decreases.

Much of the strength and hardness of the microstructure is found to come from the very small thickness of the bainite plates. It is reported that of the total strength of $2500\ MPa\ (2.5\ GPa)$ achieved by a bainitic alloy, approximately $1600\ MPa$ comes solely from the fineness of the plates. The residue of strength comes from dislocation forests, the strength of the iron lattice and solution strengthening [14, 13]. Alloys which are stronger than $1200\ MPa$ and yet possess toughness, tribological properties, favourable responses to large strain rates, resistance to fatigue, and are cheap to manufacture are usually referred to as High performance bainitic steels [11].

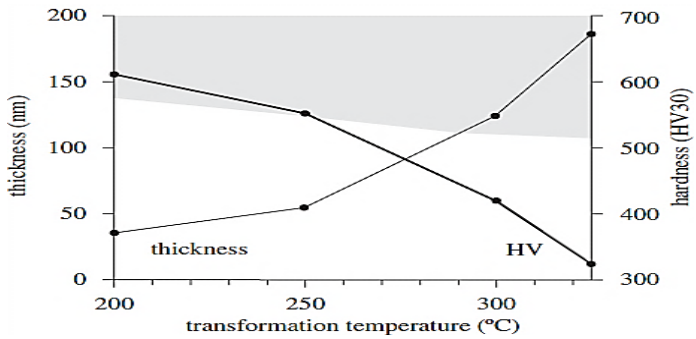

Figure 6.2: Properties of bainitic alloy system (1). The shaded region represents the fraction of austenite as a function of temperature, given by the fraction of the height of the diagram, the rest of the microstructure being bainitic ferrite [19, 36].

Transforming at low temperature to achieve finer platelets of bainitic ferrite is acclaimed to be a neat way of achieving strength without compromising toughness.

Strength increment due to dislocations is given by $\Delta\sigma \cong 7.3410^{-6}(\rho)^{0.5}$ where ρ is given in m^{-2} and $\Delta\sigma$ in MPa [36].

Figure 6.3 is the summary of the contributions of the main different strengthening mechanisms after being corrected by their corresponding ferrite volume fractions.

Figure 6.3 shows that highest strength contribution comes from the lowest transformation temperature, with 87% of bainitic ferrite present in the microstructure. The fine plate size contribute $1.6\,GPa$ while other mechanisms about $500\,MPa$. At higher transformation temperatures, the ferrite fraction decreases while its thickness increases, leading to smaller contributions from both of these strengthening mechanisms. The microstructural contributions for the $300℃$ transformed samples are only about 600 and $300\,MPa$ for plate thickness and dislocation density strengthening respectively [36].

The motivation for ever finer grain sizes comes from a desire for stronger materials. The bainitic steel has very fine grain size and could suffer from plastic instabilities upon deformation. This phenomenon reduces full exploitation of the metal strength. To avoid this retained austenite is desirable in the microstructure. The retained austenite appears between the plates of bainite each of which is thinner than a typical carbon nanotube.

Another Bainitic alloy is

$$Fe-0.79C-1.56Si-1.98Mn-0.24Mo$$
$$-1.01Cr-1.51Co-1.01Al\ wt\%$$

here referred to as **Bainitic Alloy System 2.** The major difference between this and **Alloy System 1** is replacement of $0.09V\ wt\%$ with $1.51Co\ wt\%$ and $1.01Al\ wt\%$. Cobalt and Aluminium are added to accelerate the rate of reaction by increasing the free energy difference between the ferrite and austenite phases.

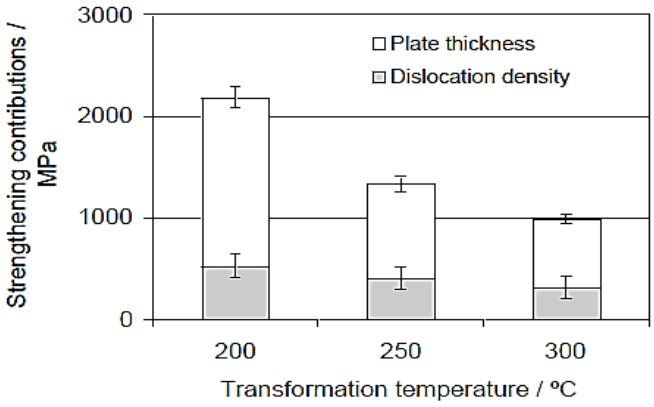

Figure 6.3: Strengthening contributions versus transformation temperature [36].

Figure 6.4 shows typical true-stress versus true-strain curves for the **Bainitic Alloy System 2** generated at $200℃$ and $300℃$. Gradual yielding characteristic of material having large number density of dislocations or a material showing transformation of some austenite during the application of stress can be seen [38].

It is noteworthy that application of stress may cause one or more of the phases to undergo transformation into an alternative structure. If this happens to produce a stronger phase then the work hardening rate of the material is enhanced. Transformation induced plasticity (TRIP) steels form a class of such steels where deformation by moving interfaces leads to greater ductility by delaying the onset of plastic instability (necking) during tensile testing.

In this **Bainitic Alloy System**, *retained* austenite is found to undergo stress- or strain-induced martensitic transformation. In other words, the austenite transforms into martensite under the influence of applied stress and this results in work hardening, with large and almost completely uniform plastic strain as shown in Figure 6.4. This capability avoids the usual considerable reduction of ductility leading to plastic instability due to development of fine-grained microstructure.

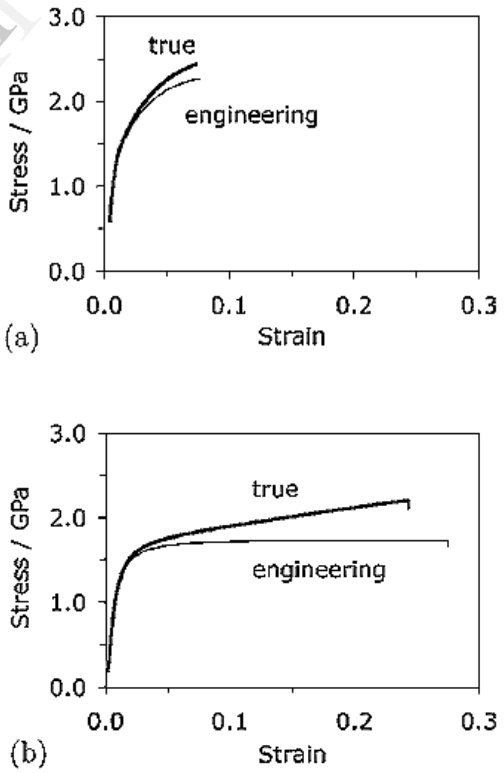

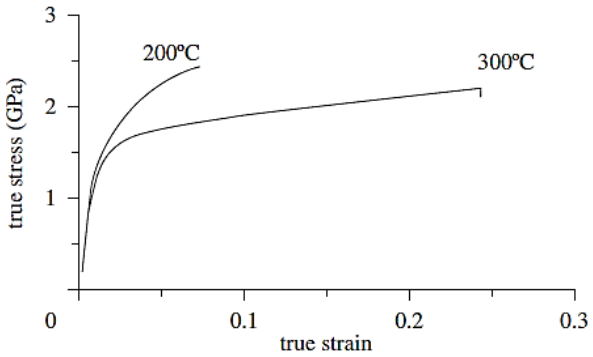

(c)

Figure 6.4: True and engineering stress–strain curves. (a) Bainite generated by transformation at 200 $^{\circ}C$. (b) Bainite generated by transformation at 300 $^{\circ}C$ (c) True stress–strain curves for transformation at 200◦C and 300◦C [19, 38].

The details of the mechanical property of the **Bainitic Alloy System 2** are listed in Table 6.1.

Another study of the mechanical properties of bainite, of the composition shown below here referred to as Bainitic Alloy System 3 was carried out at low temperature. The measured bainite and martensite transformation temperatures are also stated [36].

$$Fe-0.80C-1.59Si-2.01Mn-0.24Mo-1.00Cr$$
$$-1.51Co-0.002P-0.002S\ wt\%$$
$$M_s/^{\circ}C = 120\ and\ B_s/^{\circ}C = 360$$

The microstructure is generated by isothermal transformation at temperatures in the range $200-300^{\circ}C$. The microstructure is reported to consist of slender ferrite plates of $20-65\ nm$ thick in a matrix of carbon-enriched retained austenite. The small thickness of the ferrite plates is attributed to the increased strength of austenite at low temperatures and the magnitude of the free energy change accompanying transformation.

Table 6.1: T_I, V_γ, σ_Y and σ_{UTS} stand for isothermal transformation temperature, the volume fraction of retained austenite, the 0.2% proof and ultimate tensile strengths respectively [36].

T_I, °C	V_γ	σ_Y, GPa	σ_{UTS}, GPa	Elongation, %
200	0·17	1·41	2·26	7·6
300	0·21	1·40	1·93	9·4
400	0·37	1·25	1·7	27·5

Figure 6.5 shows the engineering stress versus strain curves of the **Bainitic Alloy System 3.** Deformation was done at room temperature and the result is a uniform plastic deformation along the gauge length of the tensile specimens. The fractured sample was reported to show little or no necking. Almost all the permanent deformation is uniform strain.

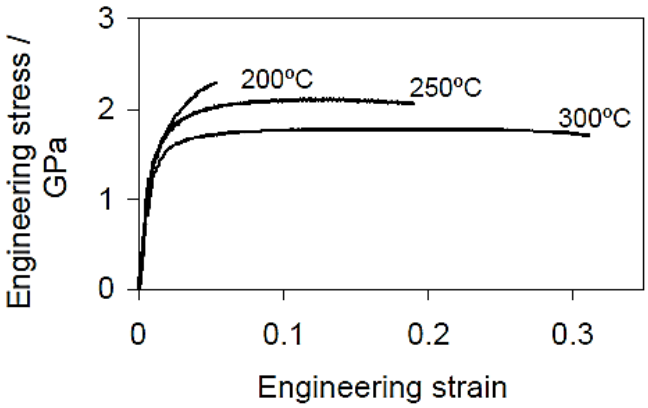

.

Figure 6.5: Stress-strain curves for room temperature tensile tests with the bainite transformation temperatures indicated [36].

It has been found that the austenite in the microstructure is the toughest phase. Fracture occurs when the austenite content V_γ approached 0.1 as shown in Figure 6.6 [19]. Fracture seems to occur when the austenite content decreases to about 10% of the microstructure.

Also plotted are points which define in each case the strain at which the tensile samples failed. A prominent feature is that they all fail when the retained austenite content is reduced or diminished to about 10%.

This microstructure was reported to possess yield strength as high as $1.5\ GPa$ and an ultimate tensile strength between $1.77-2.2\ GPa$ depending on the transformation temperature. The high strength is accompanied by ductility $\geq$ 30% and a fracture toughness $\sim 45\ MPa\ m^{0.5}$). Fig 6.7 shows how UTS, YS, total elongation and K_{IC} (fracture toughness) vary with transformation temperature.

This unusual combination of properties is attributed to the exceptionally fine scale of the carbide-free bainitic microstructure and the associated retained austenite. It can be seen that Fracture toughness, K_{IC} and ductility both decrease as the strength increases. The microstructure obtained by transformation at 300ºC was reported to possess approximately 30% elongation and fracture toughness of $44\ MPa\ m^{0.5}$. That of transformation at $200^{\circ}C$ has about 20% elongation and toughness by half of that at $300^{\circ}C$.

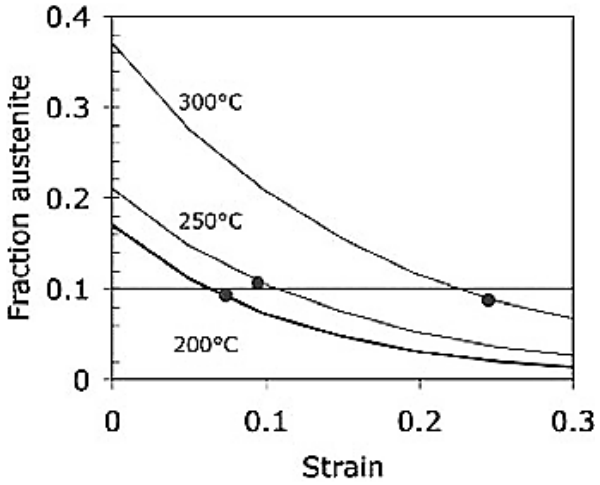

Figure 6.6: Calculated variation in the fraction of austenite as a function of plastic strain in three bainitic steels containing different initial quantities of retained austenite [19].

Figure 6.7(b) shows that the microstructure obtained at 300ºC exhibits the best results with 25% of retained austenite present after the completion of reaction, lower levels are achieved with the stronger microstructure obtained after transformation at 200ºC.

Toughness and ductility were reported to be dependent on the amount of retained austenite present in the microstructure. It is found that the bainitic ferrite fraction of the microstructure, its carbon content and dislocation density increase as the transformation temperature is reduced as shown in Fig 6.8.

Other members of this class of bainitic alloy system are shown in Table 6.2 [14, 25, 26]. They are generally referred to as $Fe - 1.5Si - 2Mn - 1C\ wt\%\ steel.$

Table 6.2: Some bainitic alloy systems

	C	Si	Mn	Mo	Cr	V	Co	Al
Alloy 1	0·98	1·46	1·89	0·26	1·26	0·09		
Alloy 2	0·83	1·57	1·98	0·24	1·02		1·54	
Alloy 3	0·78	1·49	1·95	0·24	0·97		1·60	0·99

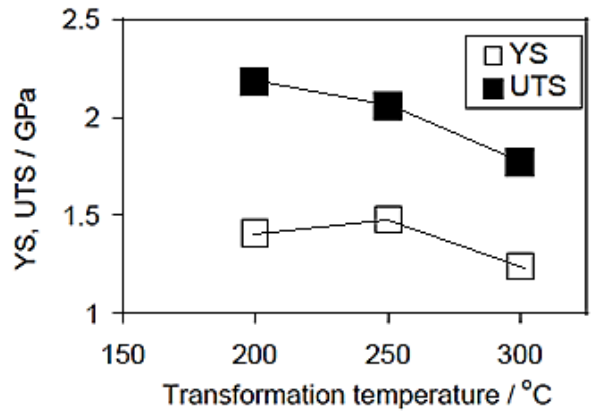

(a)

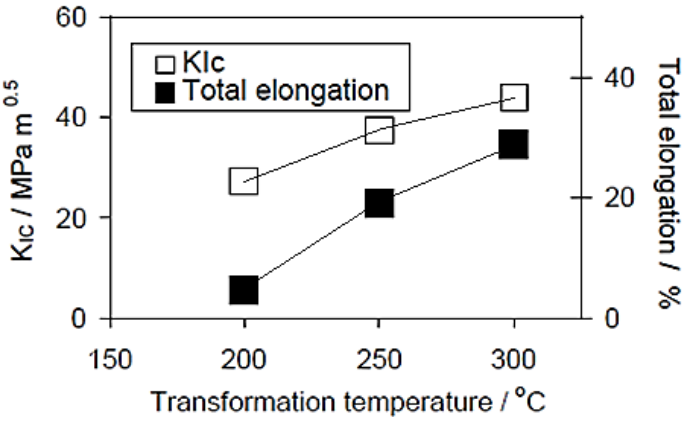

(b)

Figure 6.7: Transformation temperature dependences of UTS, YS, total elongation and K_{IC} (fracture toughness) [36].

Some of the commercially attractive features of this class of steels are [14]:

1. The bainite obtained by transformation at very low temperatures is found to be the hardest ever and has considerable ductility.
2. The ductility in this bainitic steel is found to be due to stress or strain–induced transformation of retained austenite which enhances work–hardening. The gained ductility was reported to be almost uniform under applied stress. This flexibility of steel crystalline nature makes it the commanding material for structural applications.
3. The size of the sample can be large because the time taken to reach the desired low temperature from the austenitization temperature is much less than that required to initiate bainite.
4. When combined with the inherent ability of the steel to resist pearlite formation during cooling, this means that a large steel component can be cooled slowly to B_s, thus achieving a homogeneous temperature before transformation begins in very large sections.
5. The slow cooling encourages the development of uniform properties in very large sections which helps in avoiding the development of residual stresses and hence minimizes distortion.
6. It is very cheap to produce.

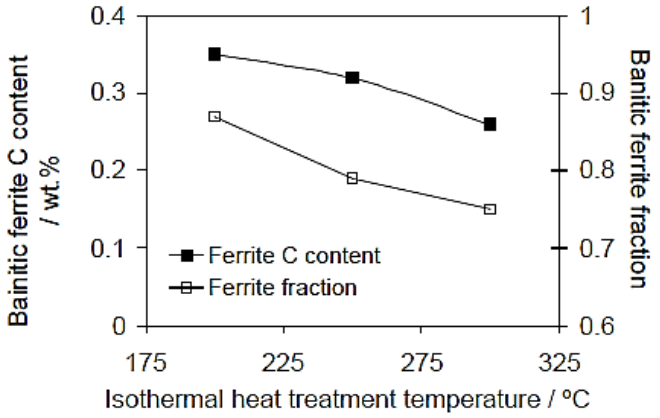

Figure 6.8: Fraction of bainitic ferrite (the remainder being retained austenite) obtained after isothermal transformation at different temperatures and times, ensuring that bainitic transformation was finished [36].

VII. Some Areas of Application of Bainitic steels

A. *Rail steel*

Rail sections are hot-rolled and continuously cooled from the austenitic state. Most of the present day rail steel is said to be pearlitic containing about $0.7\ wt\%$ carbon. The pearlitic microstructure usually consists of a mixture of soft ferrite and a hard and brittle phase called cementite (Fe_3C). The cementite is usually a product of the eutectoid decomposition of the austenite with carbon composition close to $0.8\ wt\%$. The ferrite and cementite form in alternating lamellae arrangement. The hardness increases as the interlamellar spacing decreases or as the fraction of cementite within the pearlite is made larger. Pearlite colonies can grow across austenite grain boundaries. In doing so, they destroy the structure that exists at those boundaries and remove them as potential sources for the segregation of impurity atoms such as phosphorus [11].

The pearlitic steel is believed to achieve a high resistance to wear because of the hard cementite and its containment by the more plastic ferrite. But the very cementite particles that confer hardness are also brittle. The situation is made worse by the fact that each pearlite colony is a bi-crystal. It is the size of the colony, rather than the interlamellar spacing, which defines the length scale of fracture. This property reduces drastically the toughness of a Pearlitic steel. In other words in pearlitic steels the toughness depends on the pearlite colony size, which is relatively coarse even when the interlamellar spacing is reduced. Thus, although the wear resistance can be improved by refining their microstructure, the toughness is relatively poor [11].

Fracture can occur from relatively minor stress–concentrating features inside the rail, or on its surface, as a result of manufacture or subsequent handling damage [7]. An attempt to develop better rail steel steered studies on bainite microstructure which led to the development of early bainitic steel having 70% bainite and 30% pearlite. This structure is found to exhibit unacceptable toughness and the wear on the gauge face where there is rolling–sliding contact was also worse [30].

The approximate composition of one of the recently designed bainitic carbide-free rail steel alloys is

$$Fe-0.4C-1.5Si-2.0Mn-0.25Mo\ wt\%.$$

Figure 7.1 compares the properties of the new rail steel to conventional rail steel. It is obvious that the new bainitic rails have superior wear resistance (Figure 7.1) and unlike any other rail steel, they reduce wear on the wheels [11, 31]. Tests have shown dramatic improvements in the rolling contact fatigue life. The new steels are weldable using the thermit and flash butt welding processes [11, 30, 31]. The new material exhibits these desirable properties because the high toughness contributes to wear resistance by reducing the rate of production of wear debris [11].

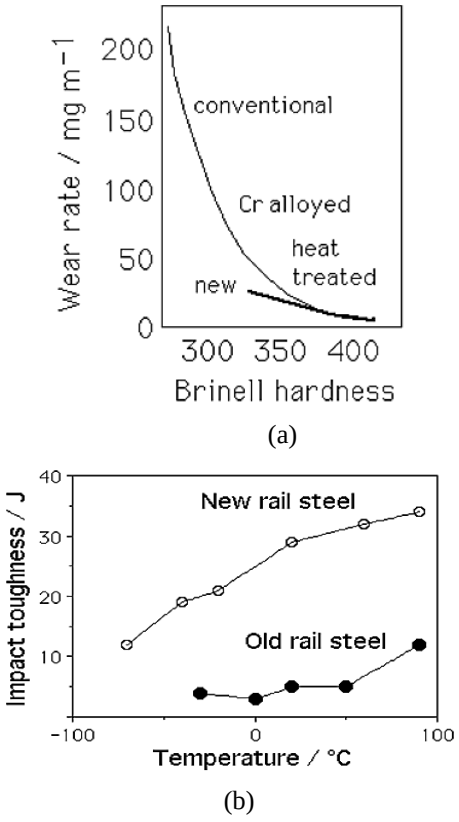

Figure 7.1: (a) Comparison of the wear rates and hardness levels of a variety of conventional rail steels against the new carbide–free bainitic steel. (b) Comparison of the Charpy toughness of new with conventional rail steel [30].

The superior property of this new steel is attributed to the presence of a softer transfer layer with high bulk hardness. During wear the material debris are produced at the contact surface followed by detachment of wear particles and transfer. The softer phase – austenite, reduces the rate of production of the wear debris. The absences of brittle cementite particles improve rolling–contact fatigue resistance.

Figure 7.2: illustrates the use of this carbide free steel. UK, Switzerland and France are reported to have applied this steel in railway construction.

Figure 7.2: Carbide-free bainitic steel in service. Swiss Railways using new rails [11].

B. *Development of Armour*

This bainite microstructure finds application in development of very strong armour. It is reported that whereas the ordinary tensile strength of the strong bainite is about 2.5 GPa, the strength can reach 10 GPa at the very high strain rates ($10^7\ s^{-1}$) associated with ballistic tests as shown in Figure 7.3.

The Bainitic Alloy system 1, transformed at 200 $^{\circ}C$ for 5 days has been used for this armour application [18]. The presence of retained austenite helps to prevent brittle failure. By transforming the steel at a higher temperature, thus multiple hits by projectile can be supported.

C. *Sheet Metal Work*

After a very demanding systematic study [39], a strong bainitic sheet metal having ultimate tensile strength of about 1400 MPa with a ductility of about 20% was produced using the data collected from reported isothermal transformation experiments on carbide–free bainite. It was produced under rapid continuous cooling process with transformation occurring over a narrow temperature range around $350°C$. The transformation time was limited to ten minutes. The data analysis was done using neural network based on a Bayesian framework. The kinetics of transformation as a function of chemical composition was also calculated. An extensive set of TTT–curve calculations were carried out in which the composition was varied systematically in the range

$$0\text{–}1Co, 1\text{–}2Cr, 1\text{–}2.5Ni, 1.2\text{–}2Mn, 0\text{–}1W\ wt\%.$$

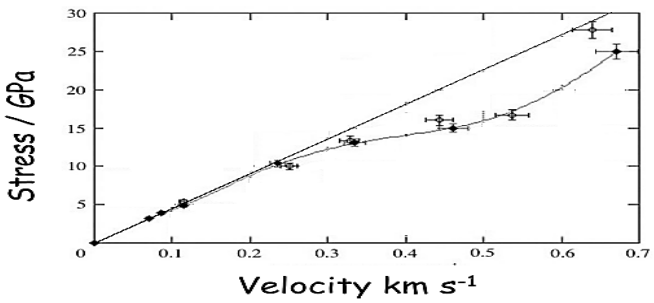

Figure 7.3: Ballistic test on the bainitic armour alloys. Departure from the straight line indicates plasticity and the horizontal axis represents projectile velocity [14, 18].

Silicon and aluminium were fixed at 1.5 and $0.5\ wt\%$ respectively in order to control cementite precipitation. Aluminium and cobalt helped to accelerate the bainite reaction. The steel chemical composition that gave favourable result was found to be

$$Fe\text{–}0.35C\text{–}1.5Si\text{–}0.5Al\text{–}0.25Mo\text{–}1.2Mn \\ \text{–}1Cr\text{–}1Ni\text{–}0.1V\text{–}1Co\text{–}1W\ wt\%$$

Subsequently, an attempt to produce this alloy gave the composition below which was close to desired alloy.

$$Fe\text{–}0.34C\text{–}1.47Si\text{–}0.54Al\text{–}0.24Mo\text{–}1.20Mn \\ \text{–}0.95Cr\text{–}0.91Ni\text{–}0.10V\text{–}1.04Co\text{–}0.99Wwt\%$$

This alloy gave the intended property - $UTS\sim 1400Mpa$ and ductility $\sim 20\%$. The properties can also be achieved by isothermal transformation for 10 minutes [39].

D. *Case hardening*

In case hardening, large concentration of carbon is diffused into the surface of low carbon steel which is then transformed into hard martensite. The hardness of wear-resistant layer developed can be as high as $750HV$ [25]. A hardness of about $800HV$ can also be achieved by quenching high carbon martensitic steel, but the dissolved carbon tends to make the martensite extremely brittle. This detrimental effect necessitates the use of low carbon steel in case carburization.

This level of hardness is reported to be possible by using this carbide-free bainite with additional advantage of toughness.

Case-carburized steel isothermally transformed at 200◦C is shown to lead to extremely fine and hard bainite $\sim 620\ HV$, in the surface layer, with the transformation inducing a compressive stress of about 200MPa into the surface [25, 40] The distortion associated with the production of the bainitic case is reported to be smaller than with the martensitic variety because of the less dramatic quench to the isothermal transformation temperature. These desirable properties of bainitic steel are yet to be explored in case-hardening technology [25].

VIII. CONCLUSION

The development of carbide free bainitic steel based on the understanding of the mechanism of transformation has been presented. No doubt enormous effort has been put in in the design of this class of steel. The possibility in bainitic steel underscores the versatility and manoeuvrability of steel crystal structure to produce outstanding materials for engineering applications. This capacity is unsurpassed by any other class of engineering materials.

REFERENCES

[1] Bhadeshia, H.K.D.H. *Some Phase Transformations in Steels.* Institute of Materials, Minerals and Mining, London, 15, 1999.
[2] Bhadeshia, H.K.D.H. *The First Bulk Nanostructured Metal*. Science and Technology of Advanced materials, doi:10.1088/1468-6996/14/1/014202, 2013.
[3] Bhadeshia, H.K.D.H. *Geometry of Crystals*. Institute of Metals, London, 1987.
[4] Bhadeshia, H.K.D.H. *Very Short and Very Long Heat-Treatments in the Processing of Steel. Materials and Manufacturing Processes.* Allied Publishers Pvt Ltd, India, 2010.
[5] Bhadeshia, H.K.D.H. *The Dimensions of Steel.* Bessemer Memorial Lecture, Institute of Materials, Minerals and Mining, London, 2007.
[6] Bhadeshia, H.K.D.H. *The Design of Strong, Tough and Affordable Engineering Alloy*. The 37th John Player Memorial Lecture, Institution of Mechanical Engineers, London, 2002.
[7] Bhadeshia, H.K.D.H. *Novel Steels for Rails*. Encyclopedia of Materials Science, Pergamon Press, Elsevier Science, ISBN 0-08-0431526, pp. 1-7, 2002.
[8] Bhadeshia, H.K.D.H. *Rationalisation of Shear Transformations in Steels.* Acta Metall. 29, 1117–1130, doi:10.1016/0001-6160(81)90063-8, 1981.
[9] Ghosh, G. & Olson, G. B. *Computational thermodynamics and kinetics of martensitic transformation*. J. Phase Equil. 22, 199–207**,** 2001.
[10] Takahashi, M. and Bhadeshia, H. K. D. H. *A Model for the Transition from Upper to Lower Bainite*. Materials Science and Technology, 6, pp. 592-603, 1990.
[11] Bhadeshia, H.K.D.H. *High Performance Bainitic Steels*. Materials Science Forum, 500-501, pp. 63-74, 2005.
[12] Bhadeshia, H.K.D.H. *Phase Transformations Contributing to the Properties of Modern Steels.* Bulletin of the Polish Academy of Sciences, 58, pp. 255 -265, 2010.
[13] Bhadeshia, H. K. D. H. *Bainite in Steels, 2nd ed.* Institute of Materials, London, 2001.
[14] Bhadeshia, H. K. D. H. *Bainitic bulk-nanocrystalline steel*. The 3rd International Conference on Advanced Structural Steels, Gyeongju, Institute for Metals, pp. 33-40, 2006.
[15] Caballero, F. G., et al. *Design of novel high-strength bainitic steels: part I.* Materials Science and Technology, 17, pp. 512-516, 2002.
[16] Caballero, F. G., et al. *Bainite in silicon steels: A New Composition-Property approach, Part I.* Materials Science and Technology, 17, pp. 512-516, 2002.
[17] Caballero, F. G., et al. *Bainite in silicon steels: A New Composition-Property approach, Part II.* Materials Science and Technology, 17, pp. 517-522, 2002.
[18] Bhadeshia, H. K. D. H. *Large chunks of very strong steel.* 52nd Hatfield Memorial Lecture, Materials Science and Technology, 21, 2005.
[19] Bhadeshia, H. K. D. H. *Nanostructured bainite.* Proceedings of Royal Society of Academy, doi:10.1098/rspa.2009.0407, 2010.
[20] Christian J W. *Theory of Transformations in Metals and Alloys, Part I.* 2nd ed., Oxford: Pergamon, 1975.
[21] Yokota, T., et al. *Formation of Nanostructured Steels by Phase Transformation.* Scripta Materialia, 51, 767-770, 2004.
[22] Caballero, F. G., et al. *Design of novel high strength bainitic steels, part 2*. Materials Science and Technology, 17, pp. 517-522, 2001.
[23] Caballero, F. G., et al. *Design of novel high strength bainitic steels, part 1*. Materials Science and Technology, 17, pp. 512–517, 2001.
[24] Caballero, F. G., et al. *Very strong, low-temperature bainite.* Materials Science and Technology, 18, pp. 279-284, 2002.
[25] Garcia-Mateo, C., et al. *Development of Hard Bainite.* ISIJ International, 43, pp. 1238–1243, 2003.
[26] Garcia-Mateo, C., et al. *Acceleration of Low-temperature Bainite.* ISIJ International, 43, pp. 1821–1825, 2003.
[27] Brown, P. M. & Baxter, D. P. *Hyper– strength bainitic steels.* Materials Science and Technology, pp. 433-438, 2004.
[28] Bhadeshia, H. K. D. H. & Edmonds, D. V. *Bainite in Silicon Steels: A New Composition-Property approach, Part I.* Metal Science, 17, pp. 411-419, 1983.
[29] Bhadeshia, H. K. D. H. & Edmonds, D. V. *Bainite in Silicon Steels: A New Composition-Property approach, Part II.* Metal Science, 17, pp. 420-425, 1983.
[30] Bhadeshia, H. K. D. H. *Novel Steels for Rails.* Encyclopaedia of Materials: Science and Technology, Elsevier Science Ltd, pp. 1-7, 2002.
[31] Yates, J. K. *Innovation in Rail Steel.* Science in Parliament, 53, pp. 2-3, 1996.
[32] Bhadeshia, H. K. D. H. *Thermodynamic Analysis of Isothermal Transformation Diagrams*. Metal Science, 16, pp. 159-165, 1982.
[33] Singh, S. B. & Bhadeshia, H. K. D. H. *Estimation of bainite plate-thickness in low-alloy steels*. Materials Science and Engineering A, 72-79, doi: 10.1016/S0921-5093(97)00701-6, 1998.
[34] Bhadeshia, H. K. D. H. & Edmonds, D. V. *The mechanism of bainite formation in steels.* Acta Metallurgia, 28, 1265-1273, pp. doi:10.1016/0001-6160(80)90082-6, 1980.
[35] Garcia-Mateo, C., et al. *Low Temperature Bainite.* Journal de Physique Colloque, 112, pp. 285-288, 2003.
[36] Garcia-Mateo, C., et al. *Mechanical properties of low-temperature bainite*. Materials Science Forum, 500-501, 495-502, 2005.
[37] Bhadeshia, H. K. D. H. *Developments in martensitic and bainitic steels: role of the shape deformation.* Materials Science and Engineering A, 378A, pp. 34-39, 2004.
[38] Garcia-Mateo, C., et al. *Role of retained austenite on tensile properties of steels with bainitic microstructures.* Materials Transactions, 46, 1839–1846, doi:10.2320/matertrans.46.1839, 2005.
[39] Sangeeta, K., et al. *Carbide–free Bainite: Compromise between Rate of Transformation and Properties.* Metallurgical and Materials A, 41, 922-929, 2010.
[40] Zhang, F. C, et al. *A novel method for the development of a low-temperature bainitic microstructure in the surface layer of low-carbon steel.* Scripta Materialla, 59, 294-296, doi:10.1016/j.scriptamat.2008.03.024, 2008.